

The lack of a common file format has been a significant barrier to the effective sharing of software tools and analysis techniques. As a solution, CXIDB is standardized on CXI files, which are based on the HDF5 format (<http://hdfgroup.org/>). In a CXI file, every measurement is represented by an entry that aims to contain all the required information for its measurement's interpretation (Fig. 1d). The entries contain several defined standardized groups that store the data along with metadata such as experimental conditions and instruments. The dictionary of defined groups can be extended to accommodate new types of metadata, and additional data (such as notebooks) can be added to the corresponding CXIDB entry in auxiliary files. Data depositors are encouraged to list publications that can be used both to cite the data entry and to document how the data were collected and processed. CXIDB includes a catalog of publicly available software to provide newcomers with a list of useful resources. The availability of high-quality software will be crucial for the progress of coherent X-ray imaging, just as it was for X-ray crystallography. The Protein Data Bank is a remarkable manifestation of such a development.

At the moment, the CXIDB stores about 6.8 million images, which represents a mere 16 hours of operation of the LCLS. With 10 million shots per day possible, and a few billion shots per day expected at the European X-ray Free-electron Laser, significant expansion of the data bank is anticipated. The data bank is open for deposition to anyone. To deposit data, contact [cxidb@cxidb.org](mailto:cxidb@cxidb.org) or visit <http://cxidb.org/>.

#### ACKNOWLEDGMENTS

I thank D. Skinner and the data contributors for helping start this project and J. Hajdu for proofreading the manuscript and providing helpful suggestions. A majority of the work in this paper was supported by the Petascale Initiative in Computational Science at the National Energy Research Scientific Computing Center (NERSC), which is funded by the US Department of Energy, Office of Science. The computational sources were provided by NERSC, which is supported by the Office of Science of the US Department of Energy under contract no. DE-AC02-05CH11231.

#### COMPETING FINANCIAL INTERESTS

The author declares no competing financial interests.

#### Filipe R N C Maia

NERSC, Lawrence Berkeley National Laboratory, Berkeley, California, USA.  
e-mail: [frmaia@lbl.gov](mailto:frmaia@lbl.gov)

1. Young, L. *et al. Nature* **466**, 56–61 (2010).
2. Seibert, M.M. *et al. Nature* **470**, 78–81 (2011).
3. Berman, H.M. *et al. Nucleic Acids Res.* **28**, 235–242 (2000).
4. Lawson, C.L. *et al. Nucleic Acids Res.* **39**, D456–D464 (2011).
5. Chapman, H.N. *et al. J. Opt. Soc. Am. A Opt. Image Sci. Vis.* **23**, 1179–1200 (2006).

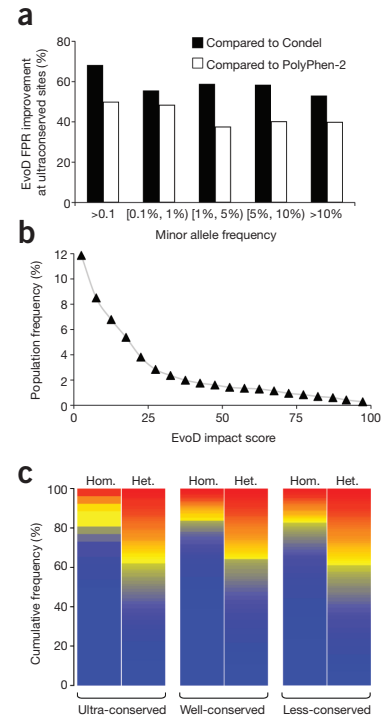
## Evolutionary diagnosis method for variants in personal exomes

**To the Editor:** Each human exome contains thousands of nonsynonymous single-nucleotide variants (nSNVs) that have unknown biological effects. The potential impact of nSNVs on biological function is now routinely assessed using computational methods for application in biomedical research and clinical genome profiling reports. Of the variants receiving a non-neutral (function-damaging) prediction, those at evolutionarily conserved sites are frequently of heightened

**Figure 1** | Performance and application of the EvoD method. (a) FPR reduction, depicted as percent improvement, for nSNVs occurring with different population frequencies at ultraconserved sites. Allele frequency data for HumVar neutral nSNVs were retrieved from the 5,400 exome data set<sup>4</sup>.

(b) The relationship of EvoD impact scores and the population frequencies of 244,272 nSNVs from the 1000 Genomes Project. The points show the average allele frequency for nSNVs with impact scores in increments of 5.

(c) Neutrality heat maps based on EvoD predictions for homozygous (Hom.) and heterozygous (Het.) nSNVs from eight HapMap exomes that occur at ultra-, well- and less-conserved sites. Heat maps were constructed by sorting nSNVs by impact score and assigning colors from dark blue (most neutral) to red (most non-neutral) on a linear scale according to the estimated *P* value.



interest for scientists and clinicians because such sites are among the most critical for proper protein function. Indeed, a majority of amino acid mutations that have been investigated experimentally are located at ultraconserved sites<sup>1</sup>, which show no amino acid residue difference among diverse species spanning over 500 million years of evolution (**Supplementary Fig. 1**). Functionally damaging mutants at these sites are likely to have significant consequences for health and disease.

For these ultraconserved sites, we estimated the false positive rate (FPR) of two state-of-the-art computational tools, Condel<sup>2</sup> and PolyPhen-2 (ref. 3), by using the standard collection of neutral variants (HumVar<sup>3</sup>) that was used to train and test these two tools (**Table 1**). Our analysis revealed a high FPR for Condel (89%) and PolyPhen-2 (75%). For 73% of the neutral nSNVs in HumVar, both produced a function-damaging prediction. Additionally, the overall accuracy of these tools at ultraconserved positions was low (55% and 60%, respectively). Therefore, predictions produced by current computational tools may mislead downstream experimental and clinical investigations aimed at studying functionally important sites.

To remedy this problem, we have developed a method that adaptively fits the best prediction model for nSNV sites evolving at distinctly different rates as revealed by multispecies comparison (ultra-, well- and less-conserved, **Supplementary Fig. 1**). Our Evolutionary Diagnosis (EvoD) method considers fundamental evolutionary properties of affected sites and amino acid changes, including measures of the biochemical severity and evolutionary probability of the amino acid change, as well as multilevel taxonomic evolutionary rates and time spans of the position affected. Within a sparse learning framework, the ability of these properties to explain the observed (training) data was evaluated in EvoD to establish an

**Table 1 | Performance of EvoD, Condel and PolyPhen-2 evaluated using the HumVar data set**

Method	Evol. consv.	HumVar: neutral		HumVar: disease associated		Diagnosis rate				Accuracy	
		True negative	False positive	False negative	True positive	TNR	FPR	FNR	TPR	BAcc	MCC
EvoD	Ultra	604	317	2,528	7,045	66%	34%	26%	74%	70%	39%
	Well	2,622	1,247	1,360	4,636	68%	32%	23%	77%	73%	45%
	Less	6,883	3,382	4,98	1,409	67%	33%	26%	74%	70%	41%
Condel	Ultra	103	818	111	9,462	11%	89%	1%	99%	55%	21%
	Well	1,500	2,369	393	5,602	39%	61%	7%	93%	66%	38%
	Less	6,183	4,082	588	1,319	60%	40%	31%	69%	65%	30%
PolyPhen-2	Ultra	226	664	556	8,552	25%	75%	6%	94%	60%	26%
	Well	2,585	1,356	1,190	4,589	66%	34%	21%	79%	73%	45%
	Less	9,398	898	1,177	625	91%	9%	65%	35%	63%	31%

Evol. consv., evolutionary conservation category; TPR, true positive rate (sensitivity); FPR, false positive rate; TNR, true negative rate (specificity); FNR, false negative rate; BAcc, balanced accuracy; MCC, Matthews correlation coefficient<sup>5</sup>. BAcc =  $\frac{1}{2}(\text{TPR} + \text{TNR})/2$ ; MCC =  $(\text{TPR} \times \text{TNR} - \text{FPR} \times \text{FNR}) / \sqrt{([\text{TPR} + \text{FPR}] \times [\text{TPR} + \text{FNR}] \times [\text{TNR} + \text{FPR}] \times [\text{TNR} + \text{FNR}])}$ .

efficient predictive statistical model (**Supplementary Methods and Supplementary Figs. 2–5**). A web server for evaluating novel variants with EvoD is available at <http://barn.asu.edu/EvoD/>.

At ultraconserved sites, EvoD led to large reductions in the FPR: 55% for Condel and 41% for PolyPhen-2. We retrieved the population allele frequency of the neutral HumVar nSNVs at ultraconserved sites from a 5,400-exome data set<sup>4</sup> and found that EvoD improved diagnoses across the spectrum of rare (<0.1%) to common (>5%) alleles (**Fig. 1a**). The balanced accuracy of EvoD was also significantly higher than that of Condel and PolyPhen-2 at ultraconserved sites (**Table 1**;  $P < 10^{-10}$ ). Furthermore, EvoD's performance was consistent across ultra-, well- and less-conserved sites, whereas Condel and PolyPhen-2 showed uneven performance across these classes (**Table 1**).

For each nSNV, the EvoD statistical model also produced an impact score that reflected the degree of neutrality: most neutral = 0 and most non-neutral = 100. In an analysis of 244,272 nSNVs from the 1000 Genomes Project, we found that the population frequency of nSNVs decayed with increasing impact score (**Fig. 1b**). We therefore used the empirical distribution of EvoD scores to determine the statistical significance of a neutral or non-neutral diagnosis ( $P$  value) adaptively for variants at ultra-, well- and less-conserved sites (**Supplementary Fig. 2**).

Using EvoD, we analyzed nSNVs in an example set of eight personal HapMap exomes<sup>5</sup> containing a total of 13,372 nSNVs at ultraconserved sites. Of these, 4% were predicted to be non-neutral ( $P < 0.05$ ). An overwhelming majority (94%) of these non-neutral nSNVs were found in heterozygous genotypes that would neutralize the negative effects of recessive alleles. Similar results were observed for 35,367 nSNVs at well- and less-conserved sites, which were also reflected in the neutrality heat maps showing the EvoD impact scores of nSNVs in heterozygous genotypes (**Fig. 1c**). In contrast, the fraction of homozygous nSNVs with high EvoD impact scores was much smaller at ultraconserved sites (**Fig. 1c**). EvoD predicted no more than one homozygous nSNV per exome to be non-neutral ( $P < 0.05$ ) in ultraconserved sites, which is consistent with the fact that individuals contributing to HapMap sequencing do not suffer from any known Mendelian disease.

Our results show that an evolution-aware approach to training and testing computational tools leads to better functional predictions for nSNVs, particularly at the most functionally important positions.

Note: Supplementary information is available at <http://www.nature.com/doifinder/10.1038/nmeth.2147>.

#### ACKNOWLEDGMENTS

We thank N. Gerek, C. Hepp and M. Champion for insightful comments and J. Akey for providing the 5,400 exomes data. C. Williams provided editorial support. This research was supported by a research grant from the National Library of Medicine (R01 LM010834) and a Postbaccalaureate Research Education Program grant (R25 GM071798) from the US National Institutes of Health.

#### COMPETING FINANCIAL INTERESTS

The authors declare no competing financial interests.

Sudhir Kumar<sup>1,2</sup>, Maxwell Sanderford<sup>1</sup>, Vanessa E Gray<sup>1</sup>, Jieping Ye<sup>1,3</sup> & Li Liu<sup>1</sup>

<sup>1</sup>Center for Evolutionary Medicine and Informatics, Biodesign Institute, Arizona State University, Tempe, Arizona, USA. <sup>2</sup>School of Life Sciences, Arizona State University, Tempe, Arizona, USA. <sup>3</sup>School of Computing, Informatics, and Decision Systems Engineering, Arizona State University, Tempe, Arizona, USA. e-mail: s.kumar@asu.edu

1. Gray, V.E., Kukurba, K.R. & Kumar, S. *Bioinformatics* (2012).
2. González-Perez, A. & Lopez-Bigas, N. *Am. J. Hum. Genet.* **88**, 440–449 (2011).
3. Adzhubei, I.A. *et al. Nat. Methods* **7**, 248–249 (2010).
4. Tennessen, J.A. *et al. Science* **337**, 64–69 (2012).
5. Ng, S.B. *et al. Nature* **461**, 272–276 (2009).
6. Matthews, B.W. *Biochim. Biophys. Acta* **405**, 442–451 (1975).

## Neonatal desensitization does not universally prevent xenograft rejection

**To the Editor:** Human cells transplanted into immunocompetent animals are generally rejected within 2–4 weeks<sup>1</sup>. Severe immune suppression is capable of protecting the grafted cells; however, such treatment is associated with unacceptable side effects<sup>2</sup>. An important advancement in the field was the introduction of immunodeficient animal models that accept xenografts, but these are poor models for human diseases<sup>3</sup>. A paper published in *Nature Methods* proposed neonatal desensitization without an overall suppression of the immune system<sup>4</sup> as an alternative. Encouraged by this study, we attempted to use neonatal desensitization to protect grafts of two types of human cells in mice and rats (**Fig. 1**). The experiments were conducted in two independent laboratories.

The first cell type we tested was immortalized, luciferase-expressing human glial-restricted precursor (hGRP) cells derived from fetal brain (Q Therapeutics). We induced neonatal desensitization by intraperitoneal injection of  $1 \times 10^5$  hGRP cells into BALB/c mice. The experiment was repeated three times using a total of 37 mice (**Supplementary Methods**). hGRPs initially